

Received 22 May 2022, accepted 14 June 2022, date of publication 27 June 2022, date of current version 6 July 2022.

Digital Object Identifier 10.1109/ACCESS.2022.3186858

Role of Flux Diverters in Reducing AC Loss in a Single-Phase 6.5 MVA HTS Traction Transformer for Chinese High-Speed Train Carrying High-Order Harmonic Currents

WENJUAN SONG¹, (Member, IEEE), ZHENAN JIANG², (Senior Member, IEEE),
MOHAMMAD YAZDANI-ASRAMI¹, (Member, IEEE), MIKE STAINES²,
RODNEY A. BADCOCK², (Senior Member, IEEE), AND JIN FANG³

¹James Watt School of Engineering, University of Glasgow, Glasgow G12 8QQ, U.K.

²Robinson Research Institute, Victoria University of Wellington, Wellington 6012, New Zealand

³School of Electrical Engineering, Beijing Jiaotong University, Beijing 100044, China

Corresponding authors: Zhenan Jiang (zhenan.jiang@vuw.ac.nz) and Wenjuan Song (wenjuan.song@glasgow.ac.uk)

This work was supported in part by the New Zealand Ministry of Business, Innovation and Employment (MBIE) the Strategic Science Investment Fund “Advanced Energy Technology Platforms” under Contract RTVU2004; and in part by the Ministry of Science and Technology (China) on the National Key Research and Development Program under Grant 2016YFE0201200.

ABSTRACT The traction transformer is a critical electrical component in high-speed-trains. We are currently building a 6.5 MVA superconducting traction transformer which will increase transformer efficiency to 99%, halve the weight, and avoid the fire risk of the conventional transformer system. AC loss from the transformer windings cannot exceed 2 kW to meet both the efficiency and weight targets. There are significant high frequency harmonics, particularly the 13th harmonic at 650 Hz, on the traction side of the transformer. Our previous work has shown the estimated AC loss in the transformer windings almost doubled with the addition of a 650 Hz harmonic current at the 8% level specified, which is not acceptable. Therefore, it is critical to reduce AC loss in the transformer due to high harmonics. In this study, we explored the role of flux diverters positioned at the outer ends of the high voltage (HV) and low voltage (LV) windings in restraining AC loss in the windings carrying high-order harmonic currents below 2 kW. Five different ring-shaped flux diverter designs were modelled in this work, utilizing the previously developed 2D axisymmetric model using the H formulation. Simulations were carried out to study the influence of the phase of the 13th harmonic, either in phase or out of phase with respect to the fundamental current, and of the inclusion of multiple harmonics on the loss. The simulation results show that placing flux diverters near the end of the windings leads to a magnetic flux distribution in the windings with reduced radial field, and hence significantly reduces the loss. Three of the flux diverter designs achieve the loss target by limiting the AC loss to below 2 kW, with a wide/thin design having the minimum weight and a wide/thick design achieving only 6% less loss, despite being almost four times heavier.

INDEX TERMS Harmonic current, AC loss, traction transformer, H formulation, flux diverter.

I. INTRODUCTION

The traction transformer is one of the essential components in Chinese Fuxing high-speed trains. The efficiency of this

The associate editor coordinating the review of this manuscript and approving it for publication was Zhouyang Ren¹.

traditional traction transformer is not greater than 96% [1], [2]. To increase the transformer efficiency and reduce the system weight and the fire risk, there have been intensive worldwide developments of superconducting transformers, which are, more efficient, lighter, and low in fire risk [3]–[15]. The present paper describes modelling results which form part

TABLE 1. Harmonic distribution in traction side of transformer.

Harmonic order	11th	13th	15th	17th
THD	3%	8%	5%	3%

of concept design development for an on-going international collaboration project aiming to develop a 6.5 MVA high temperature superconducting (HTS) traction transformer with efficiency >99% and a halved system weight of 3 tons. The project is led by Beijing Jiaotong University in China in cooperation with other parties, including Robinson Research Institute, Victoria University of Wellington in New Zealand.

AC loss of the HTS transformer is the main obstacle to the project goal and must be limited to no more than 2 kW to meet the efficiency and system weight targets [12]–[15]. In addition to the AC loss, we allow for 500 W of thermal load from current leads, bushings, and other factors [16].

The high voltage (HV) windings of the transformer are directly connected to the 50 Hz power network which contains harmonics. The low voltage (LV) windings of the transformer are connected to the traction system, which incorporates converters and switches. As a result, the current in the transformer windings has substantial harmonic content [17], [18]. According to previous reports [19], on the traction side of the high-speed train transformer, the 13th harmonic is the strongest, rather than the 3rd harmonic. Table 1 gives a typical harmonic distribution for the conventional transformer in the Fuxing high-speed train. Here, we define the total harmonic distortion (THD) for a current as

$$THD = \left(I_2^2 + I_3^2 + I_4^2 + I_5^2 + \dots \right)^{\frac{1}{2}} / I_1 \quad (1)$$

where I_k ($k = 2, 3, 4, 5, \dots$) is the RMS current of the k -th harmonic, I_1 is the RMS value of the fundamental current. In the case that a single k -th harmonic component is considered, the THD can be written as

$$THD = I_k / I_1 \quad (2)$$

As shown in Fig. 1, our previous work [19] calculated that the AC loss in the windings reaches 6.7 kW, far higher than our 2 kW AC loss limit, at the 8% 13th harmonic THD given in Table 1. Most importantly, the majority of losses was generated at the end coils of the HV and LV windings. Our earlier work [16] explored numerically the reduction of the AC loss using flux diverters (FDs) to reshape the magnetic flux distribution near the transformer windings, but that work did not consider the harmonic distortion of the current. A subsequent experimental investigation [20] demonstrated both the effectiveness of flux diverters in reducing AC loss in HTS coils and the validity of our computational methods for predicting the loss reduction. The measured results also showed negligible loss in the magnetic flux diverter materials.

In this work we explore the potential of flux diverters positioned near the end of the HV and LV windings to restrain

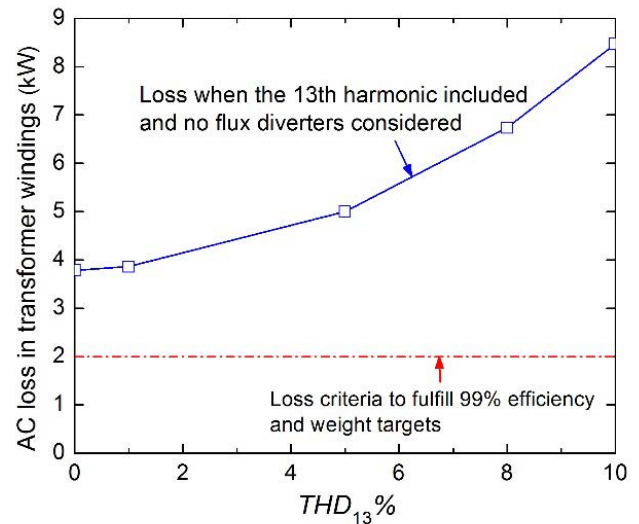


FIGURE 1. Simulated AC loss results in HTS transformer carrying rated 50 Hz current with the addition of a 13th harmonic component, plotted against THD value [10]. Here, the 13th harmonic was assumed to be in phase with the fundamental current. The dashed dotted red line denotes the 2 kW thermal criteria for both 99% efficiency and 3 tons weight.

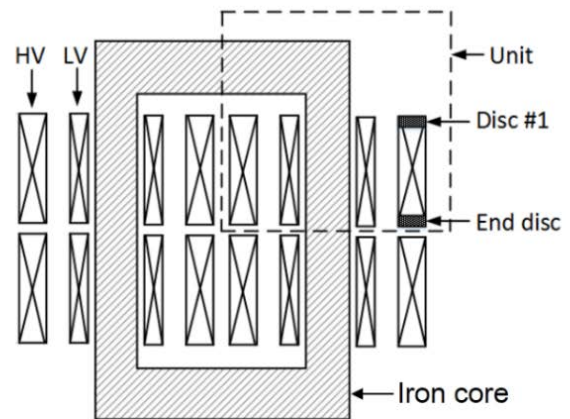


FIGURE 2. Schematic of the 6.5 MVA traction transformer structure (Only structure is indicated not electrical setup).

the AC loss below 2 kW in the transformer windings carrying current with high-order harmonic components. Various ring-shaped flux diverters designs are proposed and considered in the work, and the best of these is identified.

II. NUMERICAL SIMULATION

A. TRANSFORMER SPECIFICATIONS

Fig. 2 shows the schematic of the 6.5 MVA single-phase HTS transformer. The transformer design contains four winding units on a single iron core where each leg of the core has two winding units around it. The transformer is designed to operate at 65 K [16]. The HV winding is wound with 4 mm-wide Fujikura wire and the LV winding is wound with 8/5 (eight 5 mm wide strands) Roebel cables, assembled from punched Fujikura strands. Table 2 gives both electrical and geometrical parameters of the transformer.

TABLE 2. Design parameters in 6.5 mva traction transformer.

Electrical parameters	HV	LV
Rated voltage rms (kV)	25	1.9
Rated current amplitude, $I_{m, rated}$ (A)	91.22	1234.5
Manufacturer of tape	Fujikura	Fujikura
Wire/cable	Single wire	8/5 Roebel cable
Critical current of HTS wire (A/cm)	1140	1140
Short circuit impedance	43%	
Geometrical parameters		
Inner diameter (mm)	436.6	285
No. of turns in axial direction	116	40
No. of layers in radial direction	14	3
Total turns	1624	120
Wire/Roebel strand width (mm)	4	5
Roebel strand number	-	8
Superconducting layer thickness (μm)	1	1
Winding thickness (mm)	4.2	1.8
Unit height, L (mm)	493	488
Axial gap between two units (mm)	20	20

B. SIMULATION METHOD

AC loss simulation for the transformer was carried out in a 2D axisymmetric model, using the H formulation [21]–[23]. Homogenization method [24] was implemented in the simulation. The simulation is completed by solving the combination of Maxwell equations and E - J power law relation, the distinctive behavior of superconductors. In our previous paper [25], we verified an AC loss model for a 1 MVA transformer with its LV winding wound with Roebel cables. In this work, we adopted the same method for AC loss analysis of the 6.5 MVA transformer carrying distorted current with harmonic components.

The simulations were carried out using a 2D axisymmetric model for the transformer, as shown in Fig. 3. The radial and axial magnetic field components $\mathbf{H} = [H_r, H_z]^T$ are directly solved. Only the cross-section of the HV and LV windings in one unit is considered as schematized in Fig. 3. Superconducting windings are surrounded by an air domain. Current I flows in φ direction. The detailed modeling method can be found in our previous paper [16].

The dependence of the critical current density on the applied magnetic field is incorporated, based on measured $I_c(B)$ results divided by the cross-section area of the conductor, S . We adopted a modified Kim model [26] for the $J_c(B)$ behavior,

$$J_c(B) = \frac{I_{c0}}{S} / \left(1 + \frac{k^2 B_{para}^2 + B_{perp}^2}{B_0^2} \right)^\alpha \quad (3)$$

Fitting parameters $B_0 = 100$ mT, $k = 0.71$ and $\alpha = 0.23$ were determined by comparing fitted $I_c(B)$ curves with the measured results under perpendicular and parallel magnetic fields, as shown in Fig. 4. Here, B_\perp is the radial magnetic field B_r and $B_{//}$ is the axial magnetic field B_z .

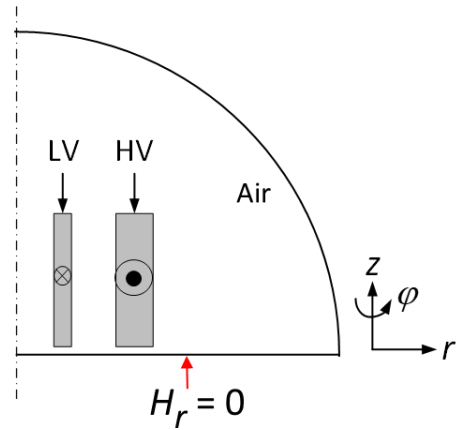


FIGURE 3. Schematic of 2D axisymmetric model for 6.5 MVA transformer (only a quarter model was simulated).

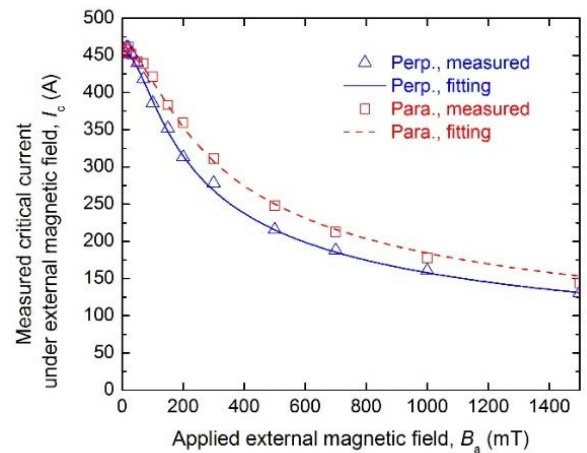


FIGURE 4. Dependence of critical current at 65 K on applied magnetic field.

The governing equations are shown below,

$$\begin{cases} \mu_0 \mu_r \frac{\partial H_r}{\partial t} - \frac{1}{r} \frac{\partial}{\partial z} \left(r \rho \left(\frac{\partial H_r}{\partial z} - \frac{\partial H_z}{\partial r} \right) \right) = 0 \\ \mu_0 \mu_r \frac{\partial H_z}{\partial t} + \frac{1}{r} \frac{\partial}{\partial r} \left(r \rho \left(\frac{\partial H_r}{\partial z} - \frac{\partial H_z}{\partial r} \right) \right) = 0 \end{cases} \quad (4)$$

where μ_0 is the magnetic permeability of the free space and μ_r is the relative magnetic permeability.

III. FLUX DIVERTER DESIGN

Fig. 5 shows the schematic of flux diverters that are positioned close to the outer end of the HV and LV windings. To be effective in shaping the flux distribution to reduce the radial magnetic field component at the end windings, the FDs need to be close to the winding ends. We assume a gap g_1 between winding ends and FD, 0.5 mm. In practice, this requires both the FDs and the outer ends of both HV and LV windings to be grounded. Our previous work [16] has shown that, at the inner end of the HV and LV windings, FDs are not required because the radial magnetic field, and hence the AC loss, is low, provided the axial gap between

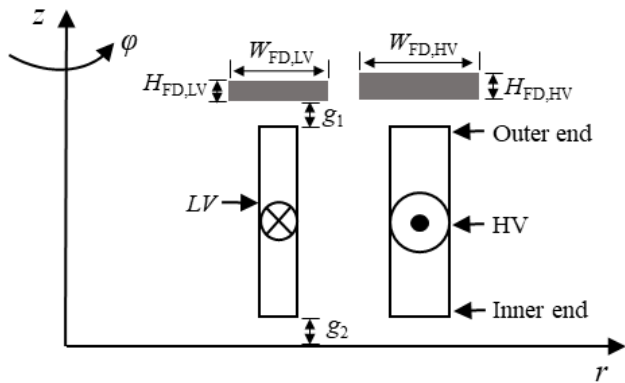


FIGURE 5. Schematic of dimensions for flux diverters at end part of windings. For better visibility, the figure is not drawn to scale.

TABLE 3. Dimensions of flux diverter designs for the transformer.

FD designs	FD in HV		FD in LV	
	$W_{FD,HV}$, mm	$H_{FD,HV}$, mm	$W_{FD,LV}$, mm	$H_{FD,LV}$, mm
FD#1	20.2	6.2	17.8	3.8
FD#2	20.2	20.2	17.8	17.8
FD#3	24.2	20.2	21.8	17.8
FD#4	28.2	20.2	25.8	17.8
FD#5	28.2	6.2	25.8	3.8

the upper and lower winding pairs on the core leg remains small. In this work we adopt an axial spacing g_2 of 20 mm. By varying the values of the width and height of the flux diverters, while keeping the radial center of the FD aligned with the radial center of the corresponding winding, five ring-shaped flux diverters are specified, as listed in Table 3, to investigate the AC loss reduction using flux diverters. The selected flux diverter material is the low-loss nickel-iron High-Flux powder-core material [27].

IV. SIMULATION RESULTS AND DISCUSSION

A. AC LOSS REDUCTION BY FDS WHEN ONLY THE 13TH HARMONIC IS CONSIDERED

Fig. 6 plots the waveforms of the distorted current in the HV and LV windings containing the 13th harmonic component with 8% THD at the rated current, as compared with the sinusoidal current waveform. It is observed that the maximum current amplitude of the resultant current with the 13th harmonic component is larger than that of the sinusoidal current. There are seven peaks or incipient peaks per half cycle in the distorted current waveform as opposed to the single peak in the pure sinusoid [20]. Each reversal of current produces additional AC loss.

The simulated AC loss values in the 6.5 MVA transformer windings using different FD designs with 8% THD of the 13th harmonic current are plotted in Fig. 7. Here, five FD designs, #1 to #5, are considered. The green dotted line shows

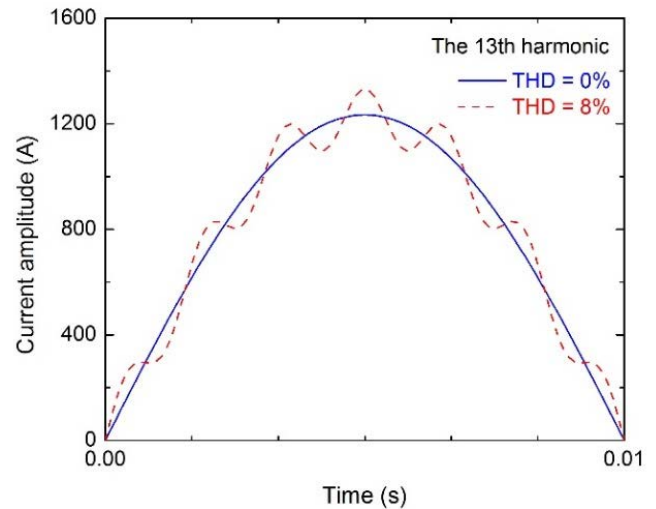


FIGURE 6. Waveforms of the current in LV winding carrying the 13th harmonic current at zero and 8% THD value, at $I_{FF,LV} = I_{rated} \cdot C1$ and $C2$: two legs of one armature coil.

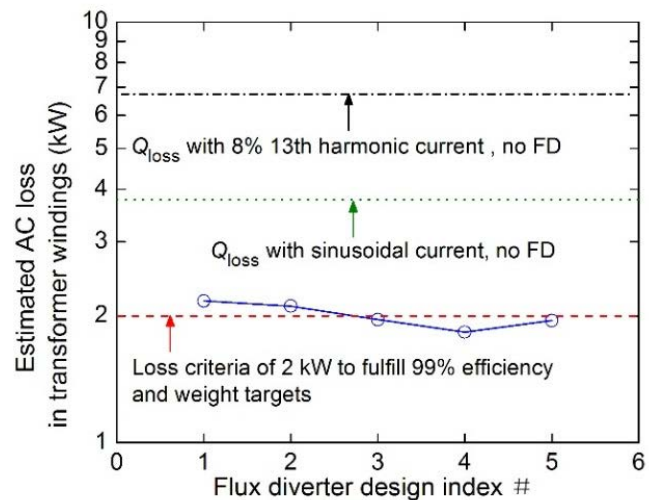


FIGURE 7. AC losses simulated with different FD designs #1 to #5, compared with that considering 8% 13th harmonic current and that considering no harmonic, at $I_{FF,LV} = I_{rated}$.

the AC loss values in the transformer winding carrying the sinusoidal rated current without FDs. The black dotted and dashed line shows the AC loss in the transformer winding with 8% 13th harmonic component without FDs. The red dashed line shows the 2 kW loss target to achieve 99% efficiency and 3 tons transformer system weight. It is obvious that flux diverters can significantly reduce the AC loss in the transformer windings. Flux diverter design #3, #4 and #5 could all limit the AC loss to below 2 kW, among which FD #4 has the maximum AC loss reduction. Note that FD #3, #4 and #5 have the same thickness, but different width. The results indicate that a wider FD will achieve more AC loss reduction.

Table 4 lists the detailed loss values in the whole transformer windings and in individual HV and LV windings, when FD #1 to #5 are used. AC loss values in the transformer

TABLE 4. Simulated AC loss values in the transformer with different flux diverter designs.

FD designs	Loss in HV, W	Loss in LV, W	Loss in Trx, kW
FD#1	370.53	170.93	2.17
FD#2	360.19	167.33	2.11
FD#3	330.77	160.37	1.96
FD#4	308.85	149.39	1.83
FD#5	331.06	156.22	1.95

windings with FD#1 and #2 were reduced to 2.17 kW and 2.11 kW, respectively, corresponding to around 68% AC loss reduction. However, AC loss values in the windings with FD#3, #4 and #5 were further reduced to 1.96 kW, 1.83 kW and 1.77 kW, respectively, which are all below the 2 kW loss target. Fig. 8 shows the simulated AC loss values in the HV and LV windings when carrying the 13th harmonic with 8% THD plotted as a function of the FD index. A similar loss reduction trend was found in the HV and LV winding.

Fig. 9 compares AC loss in each disc in the 6.5 MVA HTS transformer with/without FDs carrying sinusoidal current or current with 8% THD of the 13th harmonic at rated current. In Fig. 9(a), the loss in Disc #1 of the HV winding increases by 9% when the harmonic is added as compared to that with the sinusoidal current alone. The losses in the majority of the discs of the HV winding show obvious reduction, especially in the end discs when FD#1 and FD#5 are used, as compared to that without FDs. It is also observed that FD#5 leads to lower losses than FD#1. The indexing of the discs is indicated in Fig. 2. Fig. 9(b) indicates that there are substantial loss reductions in the LV winding as well when FD#1 and FD#5 are used, as compared to that without FDs. Again, FD#5 leads to slight better loss reduction than FD#1.

The phenomenon can be explained by the redistribution of the magnetic field in the end discs of the transformer windings when FDs are in place. Figs. 10(a)-(c) compare the radial magnetic field distribution in the HV windings at the rated current, when carrying sinusoidal current, non-sinusoidal current with 8% THD 13th harmonic component without FD, and non-sinusoidal current with 8% THD 13th harmonic component with FD#5. It is observed that the harmonic component increases the maximum radial magnetic field component, consistent with the 8% increase in peak current amplitude. This phenomenon is consistent with the findings in [28] that a larger amplitude of the current considering current harmonics will lead to higher AC losses. The flux diverters are effective in attracting the magnetic flux so that the magnetic flux lines run more parallel to the coil surface in the end discs of the windings. Figs. 10(d)-(f) compares the radial magnetic field distribution in the LV windings at the rated current, when LV carries sinusoidal

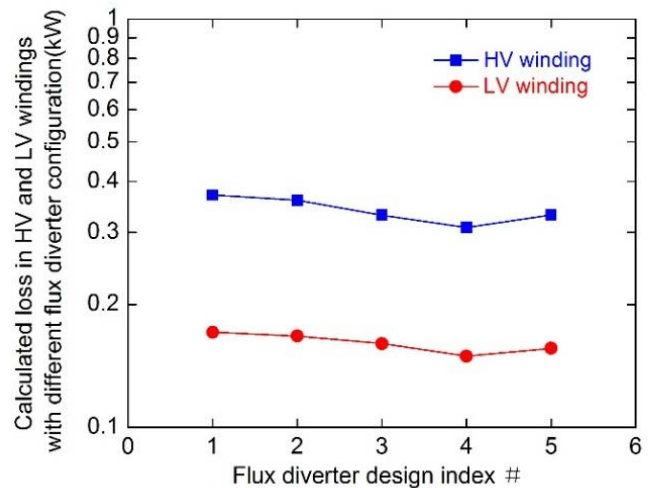


FIGURE 8. AC loss values in the individual HV and LV windings of the transformer carrying 8% 13th harmonic considering flux diverters FD #1 to #5.

current, non-sinusoidal current with 8% THD 13th harmonic component without FD, and non-sinusoidal current with 8% THD 13th harmonic component with FD#5. A similar magnetic flux reshaping effect can be observed which explains the AC loss reduction in LV windings produced by reducing the radial magnetic field around the end discs using the FDs.

B. AC LOSS REDUCTION BY FDS WHEN ONLY THE IN-PHASE AND OUT-OF-PHASE 13TH HARMONIC COMPONENT WITH REGARD TO FUNDAMENTAL CURRENT IS CONSIDERED

Fig. 11 shows waveforms for distorted currents with the 13th harmonic in-phase and out-of-phase with regard to the fundamental current, at THD = 8%. We clearly observe that the waveform with the out-of-phase 13th harmonic is notably different from that with the in-phase harmonic [29]. The current waveform with out-of-phase 13th harmonic has two peaks in amplitude leading and lagging the peak of the fundamental and 5.3% greater in amplitude than the fundamental. The maximum amplitude for the current with the in-phase harmonic coincides with the peak in the fundamental and is 8% greater in amplitude than the fundamental. The AC loss value for the transformer with in-phase 13th harmonic is slightly greater than that for the out-of-phase harmonic which is due to the difference in the amplitudes, as shown in Table 5.

Fig. 12(a) and 12(b) plot total instantaneous loss in each winding (W) through a single 50 Hz cycle, when carrying sinusoidal current, sinusoid current plus 8% in-phase 13th harmonic current, and sinusoid current plus 8% out-of-phase 13th harmonic current, at rated current. The first half cycle, during which AC current is introduced to the initially unmagnetized superconductor, differs from subsequent half cycles in which the AC magnetization distribution in the winding is established. In practice, the AC loss per cycle is given by twice the integrated instantaneous loss in the second half cycle. In Fig. 12(a), it is obvious that more peaks of

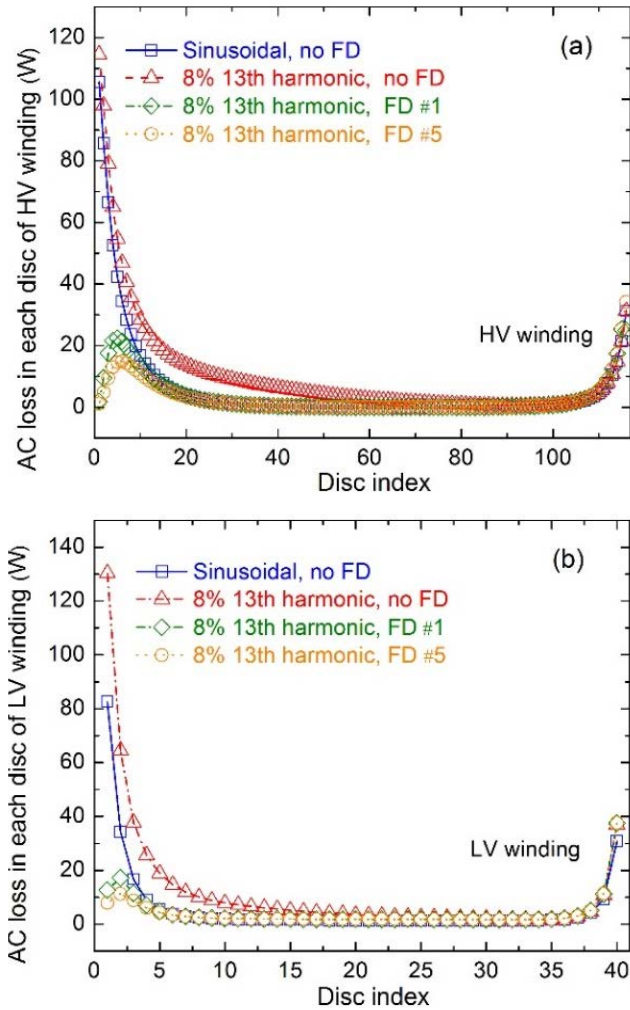


FIGURE 9. Comparison of AC loss distribution in each disc in 6.5 MVA transformer carrying pure sinusoidal current to those carrying 8% of the 13th harmonic, at rated current. (a) Discs in HV winding (b) Discs in LV winding.

instantaneous loss occur due to the resultant current waveform shown in Fig. 11, when harmonic current is considered, either in phase or out of phase, as compared to the sinusoidal case. The peaks of instantaneous loss when carrying 8% 13th harmonic current in phase occur at different times compared to those when carrying 8% 13th harmonic current out of phase. The maximum instantaneous loss peak occurs when carrying 8% 13th harmonic current in phase, consistent with the fact that it has the maximum current amplitude. The integral of the instantaneous loss for 8% 13th harmonic current in phase is greater than that for 8% 13th harmonic current out of phase. The same effect is seen in the LV winding in Fig.12(b).

C. AC LOSS REDUCTION BY FDS WHEN A HARMONIC SPECTRUM IS CONSIDERED

Fig. 13 shows the waveforms for the distorted current with multiple harmonics listed in Table 1, either in-phase or out-of-phase with regard to the fundamental current component.

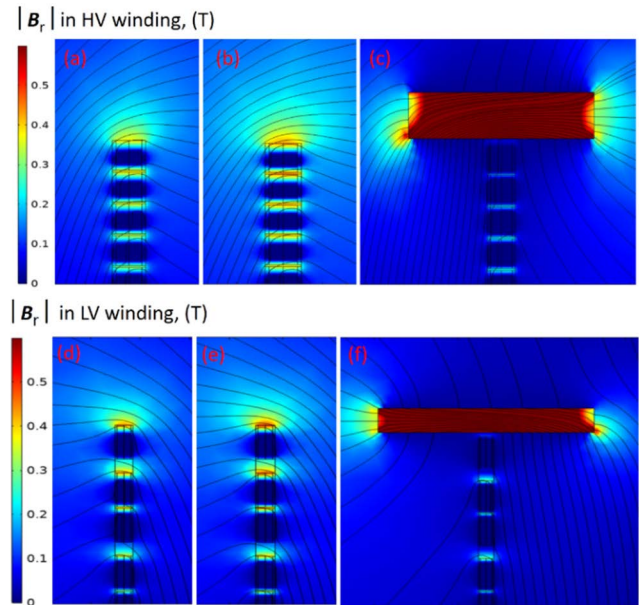


FIGURE 10. Magnetic field and flux streamline distribution in 6.5 MVA HTS transformer at rated current (a) HV, carrying sinusoidal current (b) HV, carrying 8% THD of 13th harmonic current, no FD. (c) HV, carrying 8% THD of 13th harmonic current, FD#5. (d) LV, carrying sinusoidal current. (e) LV, carrying 8% THD of 13th harmonic current, no FD. (f) LV, carrying 8% THD of the 13th harmonic current, FD#5.

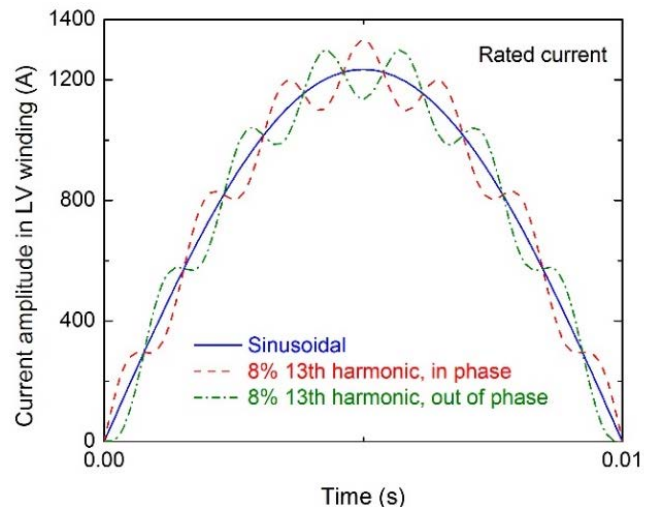


FIGURE 11. Waveforms of the current in LV winding carrying the 13th harmonic in phase and out of phase at THD = 8% and rated current.

The maximum amplitude for the current is 1271.96 A and 1249.16 A, 3.0% and 1.2%, respectively, greater than the amplitude of the fundamental. Note that FD#5 is used in the model to reduce the losses since it not only limits the AC loss to below 2 kW when carrying the single 13th harmonic but also has the smallest cross-section. As seen from the results in Table 6, with FD#5 the AC loss is limited to below 2 kW when the multiple harmonic components are either in-phase or out-of-phase with respect to the fundamental current.

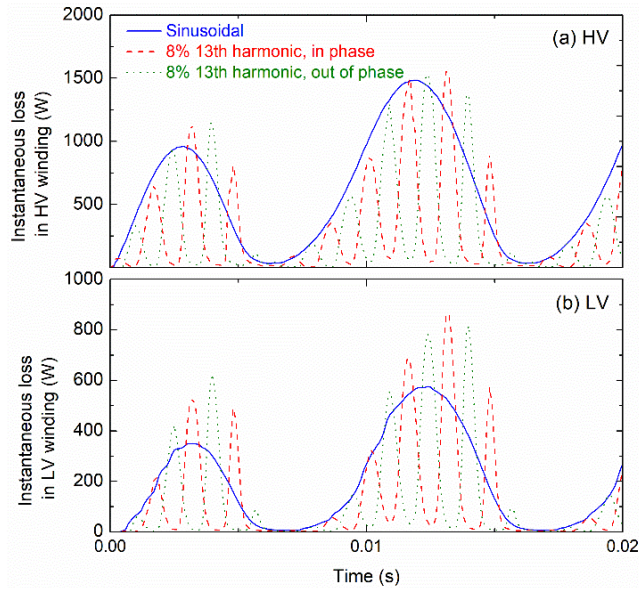


FIGURE 12. Total instantaneous loss in HV and LV windings when carrying sinusoid current without FDs, sinusoid current plus 8% in-phase 13th harmonic current with FD5, and sinusoid current plus 8% out-of-phase 13th harmonic current with FD5. (a) HV (b) LV.

TABLE 5. Loss comparison in transformer with in and out of phase harmonic.

Parameter	VALUE			
Flux diverter	NA	NA	FD5	FD5
Harmonic order	13	13	13	13
Phase	In-phase	out-of-phase	In-phase	out-of-phase
THD	8%	8%	8%	8%
Max. current (A)	1333.27	1299.62	1333.27	1299.62
Loss in HV (kW)	1.210	1.222	0.3311	0.3225
Loss in LV (kW)	0.474	0.468	0.1562	0.1511
Loss in transformer (kW)	6.74	6.76	1.95	1.89

TABLE 6. Loss comparison in transformer with sinusoidal current and multiple harmonics.

Parameter	Value	
Harmonic order	Harmonic spectrum	Harmonic spectrum
Phase	In phase	out of phase
Maximum current (A)	1271.96	1249.16
Loss in HV (kW)	0.2971	0.2969
Loss in LV (kW)	0.1356	0.1345
Loss in transformer (kW)	1.7310	1.7255

D. DISCUSSION OF SYSTEM WEIGHT AFTER ADDING THE FLUX DIVERTERS

Fig. 14 shows the weight of the flux diverters for each design. Detailed weight values can be found in Table 7. The weight m is calculated based on the volume of flux diverters V and the density of iron ρ , $m = V \cdot \rho$, as an approximation. Here, $\rho = 7.874 \text{ g/cm}^3$ was used.

As seen from Fig. 14, FD#4 has the maximum weight of 37.9 kg. FD#1 and FD#5 have relative lighter weight of

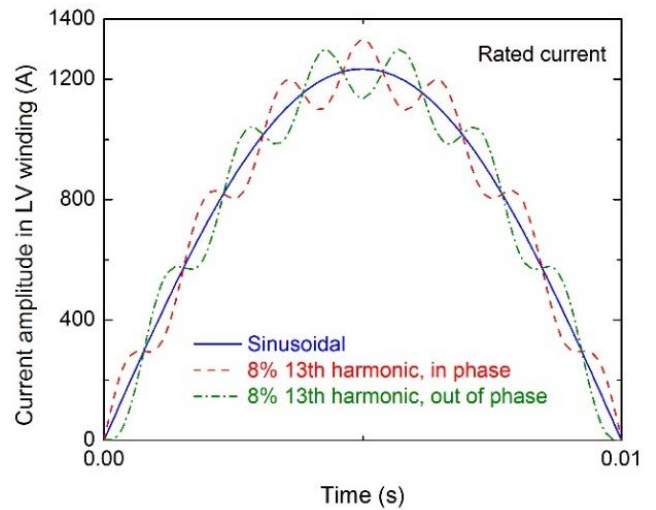


FIGURE 13. Waveforms of the current in LV winding carrying multiple harmonics together: the 11th, the 13th, the 15th, and the 17th. (The amount of each harmonic is listed in Table 1).

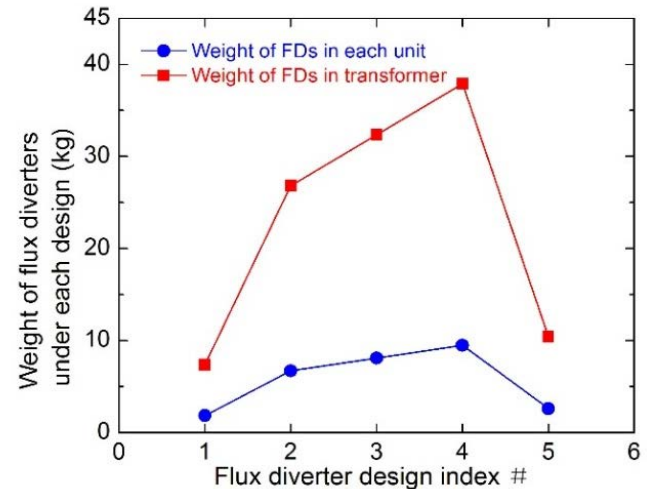


FIGURE 14. Weight of flux diverters for each design.

TABLE 7. Weight of flux diverters under different designs.

FD designs	Weight per unit, kg	Weight in a transformer, kg
FD#1	1.85	7.38
FD#2	6.70	26.80
FD#3	8.09	32.34
FD#4	9.47	37.89
FD#5	2.60	10.41

7.4 and 10.4 kg, respectively. According to Fig. 7, FD#3, #4 and #5 will meet the AC loss target of 2 kW. However, FD#5 will be a preferable option in terms of both weight and loss reduction in the transformer windings.

Table 8 shows an estimation of the weight of the system and its component parts for the required cooling power of 2.5 kW and for running times of 5 and 8 hours [16]. At 2.5 kW

TABLE 8. Estimation of system weight.

items	Values	
Running time (hours)	5	8
Cooling power (kW)	2.5	2.5
LN2 storage vessel (kg)	186	255
LN2 in storage (kg)	256	410
Pumps (kg)	230	230
Cryostats (kg)	171	171
LN2 in cryostats (kg)	452	452
Wire, formers, etc (kg)	96	96
Core (kg)	1223	1223
Flux diverters (kg)	10.41	10.41
Total for system (kg)	2632	2857

cooling power the total system after adding the weight of flux diverters still weighs less than 3000 kg even for 8 hours running time. The estimation underlines the importance of minimizing AC loss to keep the system weight within the 3-tons constraint.

V. CONCLUSION

It was evidenced by previous study that AC loss in the traction transformer windings will be significantly increased due to the harmonic current, particularly high-order harmonic. This remains a bottleneck for superconducting traction transformer application. The main contribution of this work is, for the first time, we propose to utilize flux diverters to tackle with this challenge in the traction transformer carrying high order harmonic component and harmonic spectrum, and numerical models are built to investigate the AC loss reduction by this proposal.

To constrain AC loss in the transformer windings carrying current with high-order harmonics within 2 kW, we propose to utilize flux diverters near the end of the high voltage (HV) and low voltage (LV) windings. Five different ring-shaped flux diverters were considered in this work, and AC loss calculated using a validated 2D axisymmetric model.

In this work, flux diverter rings with rectangular cross-section are considered for both HV and LV windings. The results show that using flux diverters near the end of the transformer windings leads to less perpendicular magnetic field in the end windings and hence significantly reduces the AC loss. It is obvious that the width of the flux diverters has more impact on the AC loss of the transformer winding than the thickness, and that a wider FD ring design leads to more AC loss reduction.

The simulation result shows that the addition of harmonic components distorts the current waveforms and results in higher current amplitude and hence higher AC loss in the transformer winding. The flux diverter design #5 having the smallest weight limits the AC losses in transformer windings below 2 kW, not only in the case when only the 13th harmonic

is considered, but also when the full harmonic current spectrum is considered.

The simulation results reveal that the AC loss in the transformer winding depends on the phase angle of the harmonic components, which should be considered during the design stage for accurate AC loss estimation.

The simulation results clearly show that high order harmonic components are not an insurmountable obstacle to HTS traction transformer application. Better than 99% efficiency and less than 3 tons system weight are still achievable in the HTS 6.5 MVA traction transformer fitted with low-loss flux diverters when carrying current with realistic high-order harmonic components.

ACKNOWLEDGMENT

All data is provided in full in the results section of this paper.

REFERENCES

- [1] Z. He, H. Hu, Y. Zhang, and S. Gao, "Harmonic resonance assessment to traction power-supply system considering train model in China high-speed railway," *IEEE Trans. Power Del.*, vol. 29, no. 4, pp. 1735–1743, Aug. 2014.
- [2] Z. Zhang, B. Wu, J. Kang, and L. Luo, "A multi-purpose balanced transformer for railway traction applications," *IEEE Trans. Power Del.*, vol. 24, no. 2, pp. 711–718, Apr. 2009.
- [3] H. Kamijo, H. Hata, H. Fujimoto, K. Ikeda, T. Herai, K. Sakaki, H. Yamada, Y. Sanuki, S. Yoshida, Y. Kamioka, M. Iwakuma, and K. Funaki, "Fabrication of inner secondary winding of high-Tc superconducting traction transformer for railway rolling stock," *IEEE Trans. Appl. Supercond.*, vol. 15, no. 2, pp. 1875–1878, Jun. 2005.
- [4] H. Kamijo, H. Hata, Y. Fukumoto, A. Tomioka, T. Bohno, H. Yamada, N. Ayai, K. Yamasaki, T. Kato, M. Iwakuma, and K. Funaki, "Development of low AC loss windings for superconducting traction transformer," *J. Phys., Conf.*, vol. 234, no. 3, Jun. 2010, Art. no. 032027.
- [5] Y. Wang, X. Zhao, J. Han, H. Li, Y. Guan, Q. Bao, L. Xiao, L. Lin, X. Xu, N. Song, and F. Zhang, "Development of a 630 kVA three-phase HTS transformer with amorphous alloy cores," *IEEE Trans. Appl. Supercond.*, vol. 17, no. 2, pp. 2051–2054, Jun. 2007.
- [6] M. Iwakuma, K. Sakaki, A. Tomioka, T. Miyayama, M. Konno, H. Hayashi, H. Okamoto, Y. Goshi, T. Eguchi, S. Yoshida, Y. Suzuki, H. Hirai, Y. Iijima, T. Saitoh, T. Izumi, and Y. Shiohara, "Development of a 3 ϕ -66/6.9 kV-2 MVA REBCO superconducting transformer," *IEEE Trans. Appl. Supercond.*, vol. 25, no. 3, Nov. 2015, Art. no. 5500206.
- [7] N. D. Glasson, M. P. Staines, Z. Jiang, and N. S. Allpress, "Verification testing for a 1 MVA 3-phase demonstration transformer using 2G-HTS Roebel cable," *IEEE Trans. Appl. Supercond.*, vol. 23, no. 3, Jun. 2013, Art. no. 5500206.
- [8] E. Pardo, M. Staines, Z. Jiang, and N. Glasson, "AC loss modelling and measurement of superconducting transformers with coated-conductor Roebel-cable in low-voltage winding," *Superconductor Sci. Technol.*, vol. 28, no. 11, Oct. 2015, Art. no. 114008.
- [9] M. P. Staines, Z. Jiang, N. Glasson, R. G. Buckley, and M. Pannu, "High-temperature superconducting (HTS) transformers for power grid applications," in *Superconductors in the Power Grid: Materials and Applications*, C. Rey, Ed. Amsterdam, The Netherlands: Elsevier, 2015, ch. 12.
- [10] V. S. Vysotsky, S. S. Fetisov, V. V. Zubko, S. Y. Zanein, A. A. Nosov, S. M. Ryabov, N. V. Bykovsky, G. G. Svalov, E. P. Volkov, L. S. Fleishman, and E. A. Dzhafarov, "Development and test results of HTS windings for superconducting transformer with 1 MVA rated power," *IEEE Trans. Appl. Supercond.*, vol. 27, no. 4, pp. 1–5, Jun. 2017.
- [11] M. Iwakuma, H. Hayashi, H. Okamoto, A. Tomioka, M. Konno, T. Saito, Y. Iijima, Y. Suzuki, S. Yoshida, Y. Yamada, T. Izumi, and Y. Shiohara, "Development of REBCO superconducting power transformers in Japan," *Phys. C, Supercond.*, vol. 469, nos. 15–20, pp. 1726–1732, Oct. 2009.
- [12] M. Staines, M. Yazdani-Asrami, N. Glasson, N. Allpress, L. Jolliffe, and E. Pardo, "Cooling systems for HTS transformers: Impact of cost, overload, and fault current performance expectations," in *Proc. 2nd Int. Workshop Cooling Syst. HTS Appl. (IWC-HTS)*, 2017.

- [13] A. Morandi, L. Trevisani, P. L. Ribani, M. Fabbri, L. Martini, and M. Bocchi, "Superconducting transformers: Key design aspects for power applications," *J. Phys., Conf.*, vol. 97, Feb. 2008, Art. no. 012318.
- [14] M. Iwakuma, K. Funaki, K. Kajikawa, H. Tanaka, T. Bohno, A. Tomioka, and H. Maruyama, "AC loss properties of a 1 MVA single-phase HTS power transformer," *IEEE Trans. Appl. Supercond.*, vol. 11, no. 1, pp. 1482–1485, Mar. 2001.
- [15] M. Yazdani-Asrami, M. Staines, G. Sidorov, M. Davies, J. Bailey, N. Allpress, N. Glasson, and S. A. Gholamian, "Fault current limiting traction transformer with extended fault withstand time," *Superconductor Sci. Technol.*, vol. 32, no. 3, Mar. 2019, Art. no. 035006.
- [16] W. Song, Z. Jiang, M. Staines, R. A. Badcock, S. C. Wimbush, J. Fang, and J. Zhang, "Design of a single-phase 6.5 MVA/25 kV superconducting traction transformer for the Chinese fuxing high-speed train," *Int. J. Electr. Power Energy Syst.*, vol. 119, Jul. 2020, Art. no. 105956.
- [17] M. Meinert, M. Leghissa, R. Schlosser, and H. Schmidt, "System test of a 1-MVA-HTS-transformer connected to a converter-fed drive for rail vehicles," *IEEE Trans. Appl. Supercond.*, vol. 13, no. 2, pp. 2348–2351, Jun. 2003.
- [18] M. Yazdani-Asrami, M. Mirzaie, and A. Akmal, "No-load loss calculation of distribution transformers supplied by nonsinusoidal voltage using three-dimensional finite element analysis," *Energy*, vol. 50, pp. 205–219, Feb. 2013.
- [19] W. Song, J. Fang, Z. Jiang, M. Staines, and R. Badcock, "AC loss effect of high-order harmonic currents in a single-phase 6.5 MVA HTS traction transformer," *IEEE Trans. Appl. Supercond.*, vol. 29, no. 5, pp. 1–5, Aug. 2019.
- [20] S. You, M. Staines, G. Sidorov, D. Miyagi, R. A. Badcock, N. J. Long, and Z. Jiang, "AC loss measurement and simulation in a REBCO coil assembly utilising low-loss magnetic flux diverters," *Superconductor Sci. Technol.*, vol. 33, no. 11, Nov. 2020, Art. no. 115011.
- [21] Z. Hong, A. M. Campbell, and T. A. Coombs, "Numerical solution of critical state in superconductivity by finite element software," *Supercond. Sci. Technol.*, vol. 19, p. 1246, Oct. 2006.
- [22] V. M. Rodriguez-Zermeno, N. Mijatovic, C. Traeholt, T. Zirngibl, E. Seiler, A. B. Abrahamsen, N. F. Pedersen, and M. P. Sorensen, "Towards faster FEM simulation of thin film superconductors: A multiscale approach," *IEEE Trans. Appl. Supercond.*, vol. 21, no. 3, pp. 3273–3276, Jun. 2011.
- [23] B. Shen, F. Grilli, and T. Coombs, "Review of the AC loss computation for HTS using h formulation," *Superconductor Sci. Technol.*, vol. 33, no. 3, Mar. 2020, Art. no. 033002.
- [24] V. M. R. Zermeno, A. B. Abrahamsen, N. Mijatovic, B. B. Jensen, and M. P. Sørensen, "Calculation of alternating current losses in stacks and coils made of second generation high temperature superconducting tapes for large scale applications," *J. Appl. Phys.*, vol. 114, no. 17, Nov. 2013, Art. no. 173901.
- [25] W. Song, Z. Jiang, X. Zhang, M. Staines, R. A. Badcock, J. Fang, Y. Sogabe, and N. Amemiya, "AC loss simulation in a HTS 3-Phase 1 MVA transformer using h formulation," *Cryogenics*, vol. 94, pp. 14–21, Sep. 2018.
- [26] Y. B. Kim, C. F. Hempstead, and A. R. Strnad, "Critical persistent currents in hard superconductors," *Phys. Rev. Lett.*, vol. 9, no. 7, pp. 306–312, 1962.
- [27] [Online]. Available: <https://www.mag-inc.com/Media/Magnetcs/Datash eets/C058907A2.pdf>
- [28] W. Song, J. Fang, and Z. Jiang, "Numerical AC loss analysis in HTS stack carrying nonsinusoidal transport current," *IEEE Trans. Appl. Supercond.*, vol. 29, no. 2, pp. 1–5, Mar. 2019.
- [29] M. Yazdani-Asrami, W. Song, M. Zhang, W. Yuan, and X. Pei, "AC transport loss in superconductors carrying harmonic current with different phase angles for large-scale power components," *IEEE Trans. Appl. Supercond.*, vol. 31, no. 1, pp. 1–5, Jan. 2020.

• • •